ELECTRON CYCLOTRON HEATING BY X-WAVE IN THE HSX STELLARATOR

K.M.Likin[1], A.Abdou, A.F.Almagri[1], D.T.Anderson[1], F.S.B.Anderson[1], J.Canik[1], C.Deng[2], C.W.Domier[3], S.P.Gerhardt[1], R.W.Harvey[4], H.J.Lu[1], J.Radder[1], J.N.Talmadge[1], K.Zhai[1]

[1]HSX Plasma Lab, UW-Madison, 1415 Engineering drv, Madison, WI 53706, USA
[2]Electrical Engineering Department, UCLA, Los Angeles, CA 90095, USA
[3]Department of Applied Science, UC-Davis, Davis, CA 95616, USA
[4]CompX, P.O. Box 2672, Del Mar, CA 92014, USA

e-mail: kmlikin@wisc.edu

The measurements of X-wave absorption and electron cyclotron emission on the HSX stellarator are presented. The absorption is measured with a set of microwave probes. The measured high absorption and enhanced ECE at low plasma density are due to supra-thermal electrons. Ray tracing calculations have been made for a Maxwellian plasma as well as for the added presence of a Maxwellian tail in the electron distribution function. In this bi-Maxwellian plasma, a significant fraction of the launched power can be absorbed by the tail (up to 30% in a single pass at low plasma density). The ECE temperature and the electron temperature measured by 10 channel Thomson scattering agree well with each other only at a high plasma density (>$2\cdot10^{18}$ m^{-3}). The initial results from a Fokker-Planck code, CQL3D, have been obtained.

The extraordinary wave at the second harmonic (28 GHz) produces and heats the plasma at 0.5 T in the Helically Symmetric Experiment (HSX). A distinctive feature of the quasi-helically symmetric (QHS) configuration in HSX is the reduced neoclassical transport at low collisionalities. The calculations and experiments show better single particle confinement in the QHS configuration as compared with that in mirror configurations [1,2].

A gyrotron (type VGA-8050M) is used as a microwave source with a maximum output power of 200 kW and a pulse length up to 75 msec. The main output mode is TE_{02}, which is converted along the transmission line by a series of mode converters into an HE_{11} mode. Forward and backward power is monitored with two diodes mounted on the waveguide directional coupler. The HE_{11} mode is launched from an open-ended corrugated waveguide towards the internal elliptical mirror, which focuses the wave beam at the plasma center. The X-wave cut-off density at 0.5 T is $4.8\cdot10^{18}$ m^{-3}.

In this paper, we present the results of measurements of microwave power absorption in HSX and electron cyclotron emission (ECE) spectra from the HSX plasma. The results of ray tracing calculations and calculated ECE spectra are presented as well. A bi-Maxwellian plasma model and the first run of CQL3D code for HSX parameters are discussed.

Injected power and its absorption in HSX plasma

A compact dummy load has been designed for calorimetric measurements of gyrotron power. The main elements of the dummy load are two copper plates coated with silicon carbide. By removing a short bellows at the end of the transmission line, the dummy load is positioned just before the HSX microwave window. The microwave power is then measured as a function of the beam voltage and beam current. At the HSX window, the maximum measured power is about 170 kW at 80 kV of beam voltage and 8 A of beam current. During these tests, we also measured the amplitude of signals from the microwave diodes installed on the waveguide directional coupler. From the diodes we estimate the power reflected from the dummy load and it is less than 10%. In regular operation on HSX, i.e. when the transmission line is connected to the vacuum vessel, the gyrotron power is measured with the diode on the forward shoulder of the directional coupler calibrated with the dummy load.

To measure absorption of microwave power into the HSX plasma, we use six calibrated microwave probes. Each probe consists of a standard K-band open-ended waveguide, an attenuator and a microwave diode. To get the right dynamic range in the output signal at different distances from the ECRH antenna, the attenuation varied from 60 dB (close to the ECRH launcher) down to 40 dB (far away from it). We define the multi-pass absorption coefficient as $\eta = 1 - P_{non}/P_o$, where P_{non} is the measured non-absorbed power and P_o is the power measured for a “cold” plasma discharge when the plasma density was above the cut-off. In the first experiments we put the probes around the machine at different toroidal locations in order to find out how far away from the launching antenna the power is absorbed [3]. The probes were installed at toroidal locations, which were 6°, 36°, ±69° and ±103° from the ECRH launcher. It was found that the absorption is localized within 20 cm of the ECRH antenna where the first probe was positioned. The measured efficiency at this location is about 0.9. Subsequently, we moved these six probes onto the ports next to the ECRH antenna; three probes were mounted on one side of antenna and the other three were on the opposite side. The average absorption efficiency as a function of plasma density at both toroidal locations is shown in Fig.1.

In conjunction with the measurements we also ran a ray tracing code for the 3D HSX geometry. The code has been adapted for a parallel computer and runs on a NERSC IBM RS/6000 SP computer with OpenMP and MPI constructs. The calculated single-pass absorption increases with plasma density up to $2.5\cdot10^{18}$ m^{-3} and then drops because of high refraction (Fig.2). After the reflection from the vacuum vessel wall the rays go back into the plasma. The second pass increases the total absorption from 40% up to 70% while the absorbed power profile broadens a little bit. To explain the measured high multi-pass absorption at low plasma density, the absorption on high-energy electrons should also be taken in account. We employ a model with a bi-Maxwellian electron distribution function. For this modeling we pick up a fraction of non-thermal particles and a tail tem-

perature based upon ECE measurements and stored energy from the diamagnetic loop data. Specifically, in a density scan from $0.2 \cdot 10^{18}$ m^{-3} to $1.8 \cdot 10^{18}$ m^{-3} the population of supra-thermal electrons drops from 40% to 3% and their temperature gradually deceases from 16 keV down to 1 keV. The single-pass absorption for the bi-Maxwellian plasma is shown in Fig.2. There is still a discrepancy between the measured and calculated efficiency at low plasma densities. An estimate of the additional power absorbed beyond 2 passes was made in the following manner. We pick 80 points distributed uniformly across and along the HSX vacuum vessel and from these points three rays are launched into the plasma in a random direction so that 240 rays in total simulate the bouncing power. We have found that in a wide range of plasma densities $(0.5\text{-}2) \cdot 10^{18}$ m^{-3} the multi-pass absorption can add (4 - 7)% to the total absorption. In this case the low multi-pass absorption is due to (1) the low power density in the plasma core and (2) the high ray refraction.

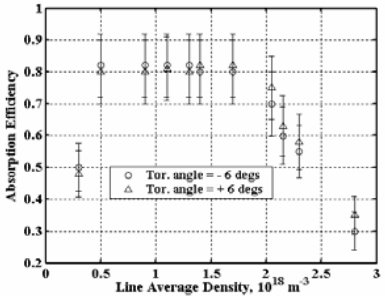

Fig.1 Measured absorption efficiency in the vicinity of ECRH antenna

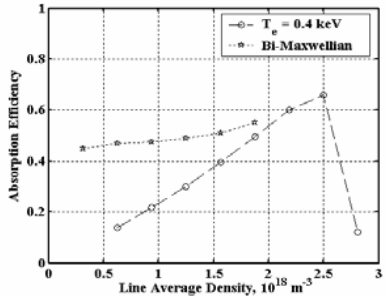

Fig.2 Calculated single-pass absorption as a function of plasma density

ECE measurements

An eight channel ECE radiometer has been implemented on HSX to measure the ECE spectrum. The detector consists of 6 channels that receive power emitted by particles on the low magnetic field side and 2 channels at the high field side. It should be noted that the spectrum of gyrotron spurious modes in up-shifted frequency band (f >28 GHz) is quite broad. At the location of the ECE horn antenna, the pick-up from the gyrotron is comparable to the plasma emission from the high field side within half of the plasma radius. At frequencies above 29.6 GHz, however, the gyrotron noise vanishes. To protect the mixer diode, a band stop filter with 60 dB insertion losses at (28±0.3) GHz and a 40 dB fast pin diode are used. The band stop filter rejects the gyrotron power at 28 GHz. The fast pin diode eliminates the spurious modes generated at the leading edge of the gyrotron pulse and whose spectrum is beyond the band of the notch filter. A 20 mW local oscillator at 42.5 GHz is attached to a mixer diode. After the mixer diode, the IF signal is amplified by two amplifiers with a total gain of 50 dB. Then it is split by an 8-way divider and goes through the narrow band (200 and 400 MHz) filters followed by a crystal detector (HP 8472) and 20 dB video amplifier. The radiometer has been absolutely calibrated on a bench. The sensitivity of different channels is in the range of (10 – 20) V/μW.

The radiated temperature is obtained by multiplication of the raw signal with a calibration factor that includes the sensitivity of each channel and the étendue of the horn antenna assuming that the plasma is a black body. The ECE temperature from every channel drops with the plasma density. A comparison between the electron temperature measured by Thomson scattering at r/a =0.2 and the ECE temperature at the same radius on the low magnetic field side is presented in Fig.3. One can see that both temperatures are close to each other only at a high plasma density. To calculate the ECE spectrum we use a bi-Maxwellian plasma model [4].

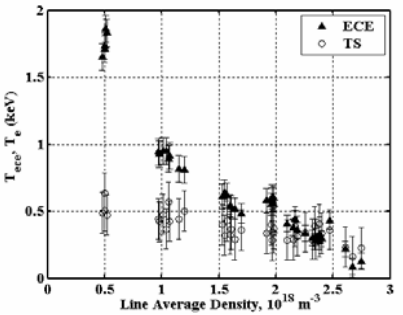

Fig.3 ECE and Thomson scattering temperatures at $r/a_p = 0.2$ as a function of plasma density

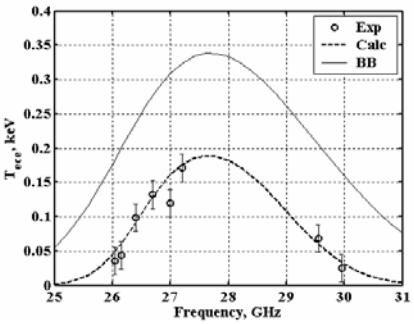

Fig.4 ECE spectrum at high plasma density (solid line if plasma was a black body)

At a line average density of $2.5 \cdot 10^{18}$ m^{-3}, the ECE spectrum has only a thermal component (Fig.4). To estimate an optical depth at different frequencies we use Thomson scattering and interferometer data with the following fit functions: $T_e = 0.33 \cdot \exp(-3r^2)$ (in keV) and $n_e = 3.5 \cdot \exp(-2r^3)$ (in 10^{18} m^{-3}). In these calculations the optical depth at the perpendicular sight view has been found and we employ the simple formula $T_{ece} = T_e \cdot (1-\exp(-\tau))$ to calculate the ECE temperature. The measured spectral points and calculated ECE spectrum are in a good agreement.

When we lower the density the emission increases on the low field side first and then on the high field side as well (Fig.5). Figure 6 represents the ECE spectrum at $0.5 \cdot 10^{18}$ m^{-3}. At a low plasma density, when the optical depth of the bulk plasma is low, the emission is entirely determined by supra-thermal electrons. In HSX at the magnetic field of 0.5 T on the plasma axis the heating occurs in a narrow central region. It is expected that the supra-thermal electrons are localized mostly in this central region. For a perpendicular sight view, the emission from these electrons is downshifted to the low magnetic field side due to a relativistic mass increase, in another words, the emission is asymmetric with respect to the resonant magnetic field. So at perpendicular detection the enhanced ECE signal

at the higher frequencies can be due to a broad profile of supra-thermal particles. In this case it is unlikely to detect a high peak at the low frequencies. On the other hand, a cyclotron absorption shape is symmetric at smaller propagation angles (< 65 degrees) and the supra-thermal electrons in the central region can make some contribution to the high frequency part of ECE spectrum. In HSX in terms of the wave pattern of receiving antenna and the geometry of the port, where the antenna is mounted, emission at perpendicular and oblique propagation directions is worth considering. Let us assume that the horn antenna receives a non-thermal electron emission mainly at 90 and 60 degrees and define the radiated temperature as a sum of two terms: $T_{ece} = T_1 \cdot (1-\exp(-\tau_1)) + T_2 \cdot (1-\exp(-\tau_2))$, where T_1, T_2 and τ_1, τ_2 are the "temperature" of the tail and the optical depth along the perpendicular and oblique sight views, respectively. Then we calculate the optical depth of each components and the radiated temperature. The best fit we found between the calculated and measured spectrum is with the following profiles: $T_1=6\cdot\exp[-8\cdot(x+0.1)^2]$, $T_2=12\cdot\exp[-8\cdot(x+0.4)^2]$, $n_1=0.15\cdot\exp(-6\cdot|x+0.1|^3)$, $n_2=0.25\cdot\exp(-6\cdot|x+0.4|^3)$, where T_1,T_2 in keV and n_1,n_2 in 10^{18} m^{-3}, and x is the effective plasma radius. This estimate gives about 30% population of supra-thermal electrons (Fig.6). In order to estimate the ECE spectrum more accurately we need to know the electron distribution function.

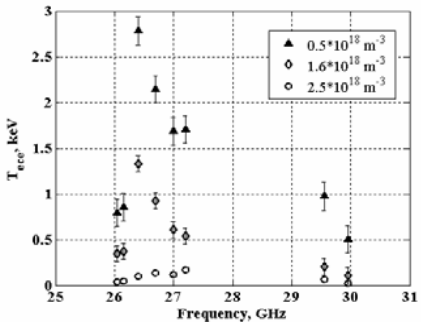

Fig.5 ECE spectrum at different plasma densities

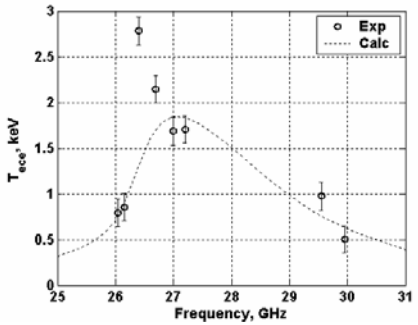

Fig.6 ECE spectrum at low plasma density

CQL3D code for HSX plasma

CQL3D is a Fokker-Plank code with one dimension in plasma coordinates and two dimensions in a momentum space, i.e. radius of the flux surface and the parallel and perpendicular components of velocity, respectively [5]. The code was developed for a tokamak geometry. At the location of the ECRH antenna the mod-B contours look tokamak-like and the CQL3D code can simulate the electron distribution function during ECRH.

The first run of CQL3D code for an HSX plasma has been done at a central density of $3\cdot10^{18}$ m^{-3} and 100 kW of launched power. It is seen that a significant distortion of the electron distribution function occurs in the energy range of 5-15 keV (Fig.7). Figure 8 shows the absorbed power profile used in CQL3D code (in this case, total absorbed power is about 10 kW). Further work is necessary in order to calculate the distribution function for different HSX operating regimes.

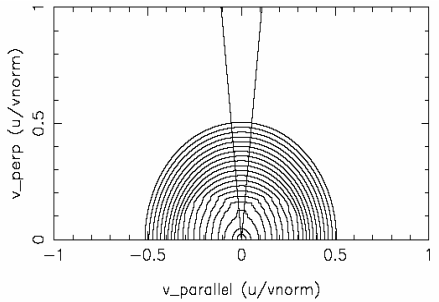

Fig.7 Contour plot from CQL3D code at rho = 0.05 (u_{norm} = 50 keV)

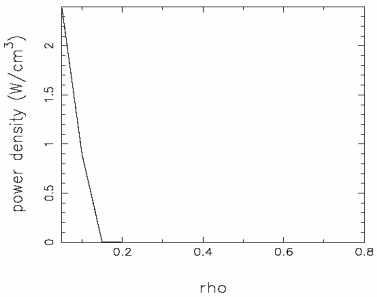

Fig.8 Absorbed power profile used in CQL3D code

Summary

We have measured the multi-pass absorption efficiency of X-wave into HSX plasma with a set of microwave probes. The absorption stays very high (~0.8) over a wide range of plasma densities. The first ECE measurements have been made. A high non-thermal feature in the ECE spectrum at a low plasma density has been measured while the spectrum at a plasma density higher than $2\cdot10^{18}$ m^{-3} is thermal. Intensive ray tracing calculations in a bi-Maxwellian plasma shows that the presence of supra-thermal electrons at a low plasma density can partly explain the high absorption and enhanced EC emission. At a high plasma density, the ECE temperature is close to that measured by Thomson scattering. First runs from the CQL3D code have been made for HSX parameters.

Acknowledgments

The work is supported by DOE grant #DE-FG02-93ER54222.

References

[1] K.M.Likin, et.al. Plasma Phys. Contr. Fusion, 2003, **12A**, A133
[2] J.N.Talmadge, et.al. Fusion Science and Technology, 2004 (accepted)
[3] K.M.Likin, et.al. Radio Frequency Power in Plasmas, 2003, **694**, 331
[4] M.Bornatici and F.Engelmann, Phys.Plasmas, 1994, **1** , 189
[5] R.W.Harvey and F.W.Perkins, Nucl. Fusion, 1997, **37**, 69